

Penetration Depth of Near-Infrared Light in Small, Thin-Skin Watermelon

Man Qian^{1,2,3,4,5}, Qingyan Wang^{2,3,4,5}, Liping Chen^{1,2,3,4,5(✉)}, Wenqian Huang^{2,3,4,5},
Shuxiang Fan^{1,2,3,4,5}, and Baohua Zhang^{2,3,4,5}

¹ Beijing Research Center of Intelligent Equipment for Agriculture, Beijing 100097, China
qianman101504@163.com, fanshuxiang8903@163.com

² National Research Center of Intelligent Equipment for Agriculture, Beijing 100097, China
{wangqy, chenlp, huangwq}@nercita.org.cn

³ Key Laboratory of Agri-Informatics, Ministry of Agriculture, Beijing 100097, China

⁴ Beijing Key Laboratory of Intelligent Equipment Technology for Agriculture,
Beijing 100097, China

⁵ College of Mechanical and Electronic Engineering,
Northwest Agricultural and Forestry University, Yangling 712100, Shanxi, China
zhangbaohua@sjtu.edu.cn

Abstract. Non-destructive detection of internal quality in watermelon has very important significance for improving watermelon's production efficiency. Near-infrared (NIR) spectroscopy is one of the most popular non-destructive detection methods. However, it is challenging to collect spectra exactly due to the multiple scattering and absorbing by the skin and internal tissues. In order to obtain the interactions between light and watermelon tissues, the transportation feature of NIR light in small, thin-skin watermelon was studied in the range of 750–900 nm. For this purpose, the diffused transmission spectra were collected with removing the sample slices along the perpendicular bisector of the source-detector line. Based on the spectra in effective wavelength band, the penetration depth curves were fitted by least square method, and the results of different detecting positions (equator and top) were compared. It was shown that, light penetration depth on the equator was 8.3–9.5 mm, 8.7–17.8 mm and 18.9–38.5 mm with source-detector distance of 10 mm, 20 mm and 30 mm, respectively. The penetration depth on the top was less than the equator. And the penetration depth increased with source-detector distance increasing. With deeper penetration depth, more information about internal quality was carried by the diffused transmission spectra. However, the intensity of spectra was weaker. According to these results, a reasonable source-detector distance could be designed for collecting effective information about internal quality. This study is of potential significance for optimizing the handheld probe geometry for large fruit, and offers theoretical bases for non-destructive detection.

Keywords: Near-infrared spectroscopy · Penetration depth · Transportation features · Diffused transmission spectra · Small, thin-skin watermelon

1 Introduction

Watermelon is one of the most popular fruits in summer, and its consumption is large. With the development of consumer's demand for fruit's quality, more attention have been paid to the internal quality, including soluble solid content, taste and nutritional value. And high internal quality can enhance the competition of domestic watermelon. However, due to the excessive watering and unreasonable fertilization, the quality of watermelon has fallen down with increasing planting area in recent years. Therefore, it is important to detect watermelon's internal quality at the postharvest handling and processing stage. However, the traditional detection method which mainly depends on destructive sampling is inefficient. It also cannot be applied widely. And it is urgent to develop a fast and non-destructive detection method to improve watermelon's internal quality.

Near-infrared spectroscopy has many advantages, including efficient analysis, fast execution, reproducibility and without sample pre-processing. And it plays a vital role in non-destructive and fast detection for fruits and vegetables. Near-infrared spectroscopy has already been used to detect watermelon's quality, such as firmness [1], soluble solids content [2–4] and maturity [5, 6]. And near-infrared spectroscopy with diffused transmission is more suitable for developing portable detecting system. Therefore, it is significant to acquire the transmission features and penetration depth of NIR light in watermelon's tissue. Many researches on light penetration depth in fruit have been reported by domestic and foreign scholars. The light penetration depth in fruit can be estimated by using the coefficient of absorption and reduced scattering [7]. The direct experimental measurement includes using a black knife to hinder light penetrating into the fruit [8], removing the sample slices gradually [9, 10] and piercing the fruit by optical probe to measure directly [11]. However, the research subjects are small fruits, such as apples, oranges, mandarins, tomatoes or pears. And researches on larger fruits have been rarely reported, such as watermelons.

To solve this problem, in this paper the diffused transmission spectra were collected, which were fitted by partial least square (PLS) method. Then the penetration depth on the equator and top were obtained with different source-detector distance (10 mm, 20 mm and 30 mm). And a suitable source-detector distance could be designed to reach effective transmission depth in watermelon. It provided technical basis for developing portable and non-destructive detection equipment for large fruits.

2 Materials and Methods

2.1 Fruit Samples

In this work, two small, thin-skin watermelons (Te Xiaofeng) were purchased from a fruit shop in Beijing. The vertical and horizontal diameters of watermelon are about 120 mm. And there are few defects on watermelon's surface. And they were placed in the room condition (20°C) for more than 24 h to avoid the influence of temperature on the detection results. The detective positions have no defects, and the light intensity can't

destruct watermelon's tissue. The samples were labeled to detect the penetration depth for the equator and top, respectively.

2.2 The System Setup and Diffused Transmission Spectra Collection

Figure 1 illustrates the experimental setup. The system for collecting spectra included a halogen lamp (Illumination Technology, 50 w), portable Near-infrared spectrometer (USB 2000+, Ocean Optics, US, 500–1100 nm), probe of optical fiber (Ocean Optics, US), fruit holder and computer. The spectrometer's resolution is 1.7 nm and integral time is 2 s. In order to avoid stray light, the fiber probe, watermelon sample and fruit holder were placed in the black light box. Meanwhile, the source fiber probe and detector fiber probe aimed at the labeled detective position, tightly. Then the diffused transmission spectra could be collected.

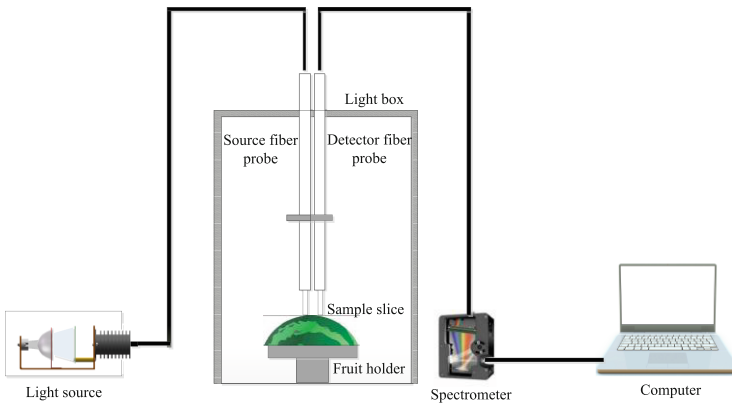


Fig. 1. Illustration of spectra collection system

Figure 2a shows the illustration of spectra collection. The spectra were collected with removing the sample slices along the perpendicular bisector of the source-detector line on the basis that the light transmission path is “banana-shaped” between the source and detector [12]. Figure 2b shows the position of source fiber probe and detection fiber probe, including 1, 2, 3 source points and 1', 2', 3' detection points. The distance between source and detector is 10 mm, 20 mm, 30 mm, respectively.

The half of watermelon was used as the original melon slice for spectra collection because of the light penetration depth less than half a watermelon. The spectra of each thickness slice were collected with different source-detector distance until the thickness is about 1 mm. The slice thickness values were 57.9, 45.8, 30.4, 23.3, 13.6, 11.3, 7.5, 5.6, 3.4, 1.2 mm. The spectra were collected for 5 times on the same position for each thickness slice, and the average spectrum of five times was used to analyze transportation features and penetration depth.

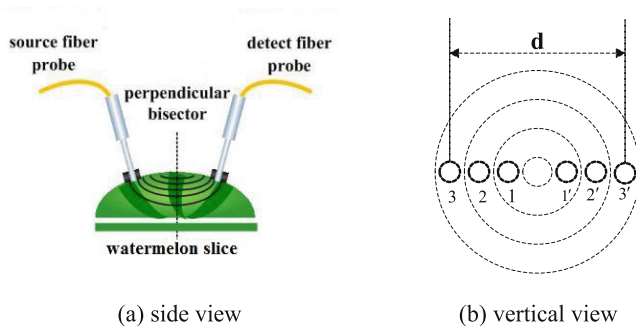


Fig. 2. Illustration of collecting spectra

2.3 Spectral Data Preprocessing and Analysis

2.3.1 Spectral Data Preprocessing

In this study, Savitzky-Golay was used to smooth the original spectra. The processing window was 7 and calculation time was 3. After Savitzky-Golay preprocessing, the feature information was strengthened and random noise was weakened.

2.3.2 Light Penetration Depth for Single Wavelength

For each wavelength (λ), the spectra of thickest slice are the reference spectra (I_1) to the spectra ($I_n, n = 1, 2, \dots, 10$) of each thickness slice ($\delta_n, n = 1, 2, \dots, 10, \delta_1 > \delta_2 > \dots > \delta_{10}$), called $g_n = \frac{I_1}{I_n}, n = 1, 2, \dots, 10$ are compared.

Then a non-linear model of the form $g_n = 1 + a \cdot \exp(b, \delta_n)$, with the parameter of a, b . And g_n (the I_1/I_n ratio) is the fitted value. δ_n (the thickness of watermelon slice) is fitted to measured points, using the least squares method. Then $\delta_1/0.1$ points of the fitted curve are taken, and the step length is 0.1 on the horizontal ordinate. An infinitesimal ε is given. A certain point $[\delta(x), g(x)]$ to neighboring point $[\delta(x + \delta_1/0.1), g(x + \delta_1/0.1)]$ is compared. If $[g(x + \delta_1/0.1) - g(x)]^2 < \varepsilon$, the value of x is approximately penetration depth of the wavelength (λ).

2.3.3 Light Penetration Depth in Effective Wavelength Range

Because the NIR light in 750–900 nm is low absorption and high scattered in biological tissues, the light can penetrate several centimeters in the tissues [13]. Due to the systematic error and random noise, the wavelength range in 750–900 nm is to analyze penetration depth, and the step length is 20 nm. For each wavelength, the penetration depth was fitted by least square method as the single wavelength.

3 Results and Discussion

3.1 Features of NIR Spectra

Figure 3 shows the diffused transmission spectra with varying thickness on the equator when source-detector distance is 10 mm. Due to the high relative transmission and low reflectance, the spectra of the thinnest slice are at the bottom. The spectra of thicker slices are on the top. When the slice thickness is 7.5 mm, the intensity of spectra fell significantly. It indicates that the NIR light transmit the slice and the penetration depth is about 7.5 mm. When the slice thickness is less than or equal to the penetration depth, light will transmit the slice and thus reflect less. The signal to noise ratio is lower with further source-detector distance and the light transportation features make little difference on the equator and top.

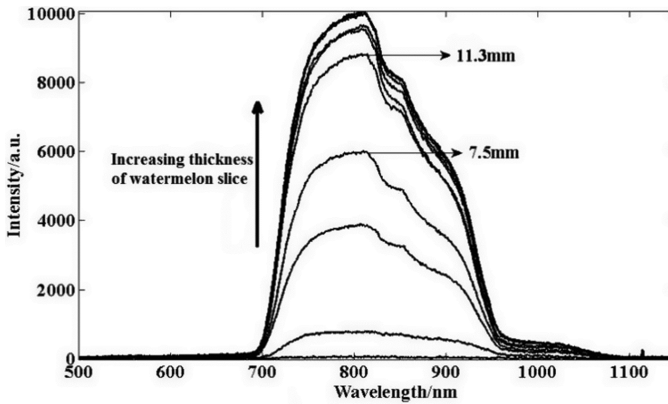


Fig. 3. The diffused transmission spectra with source-detector distance of 10 mm on the equator

3.2 The Penetration Depth for Single Wavelength

Figure 4 shows the fitted penetration depth curve for peak wavelength. When source-detector distance is 10 mm, the penetration depth is 8.4 mm on the equator. Table 1 shows the penetration depth of peak wavelength with different source-detector distance on the equator and top. As shown in Table 2, the maximum penetration depth is 29.8 mm and 21.1 mm on the equator and top with 30 mm source-detector distance, respectively. And the minimum penetration depth is 8.4 mm and 8.3 mm on the equator and top with 10 mm source-detector distance, respectively. It is noticed that the penetration depth is deeper with further source-detector distance on the equator and top. Meanwhile, the penetration depth on the top is less than the equator.

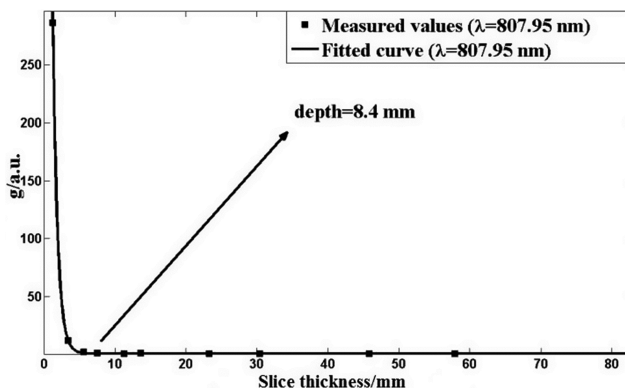


Fig. 4. The fitted curve of penetration depth for single wavelength

Table 1. Penetration depth for peak wavelength

Position	d (mm)	Peak wavelength (nm)	Penetration depth (mm)
Equator	10	807.95	8.4
	20	804.33	14.5
	30	793.46	29.8
Top	10	810.24	8.3
	20	804.00	13.2
	30	806.63	21.1

Table 2. Penetration depth in effective wavelength range

Position	d (mm)	Wavelength to largest penetration depth (nm)	Penetration depth range (mm)
Equator	10	755.26	8.3–9.5
	20	754.14	8.7–17.8
	30	770.21	18.9–38.5
Top	10	754.14	8.5–9.3
	20	757.50	7.2–15.6
	30	757.50	8.4–31.2

3.3 The Penetration Depth in Effective Wavelength Range

Figure 5 shows the penetration depth curves in effective wavelength band. On the equator, the penetration depth is nearly 10 mm with source-detector distance of 10 mm and the penetration depth curve is less volatile. It is because that the NIR light is mainly scattered due to the low penetration depth. The penetration depth is 8.7–17.8 mm and 18.9–38.5 mm with source-detector distance of 20 mm and 30 mm, respectively. Because the slice absorbs more and optical energy decreases with wavelength

increasing, the penetration depth falls down. The transportation features make little difference on the equator and top. And the penetration depth on the top is less than the equator. It is probably due to less soluble solid content and more water in the top than the equator. The slice absorbs more and the penetration depth is less on the top.

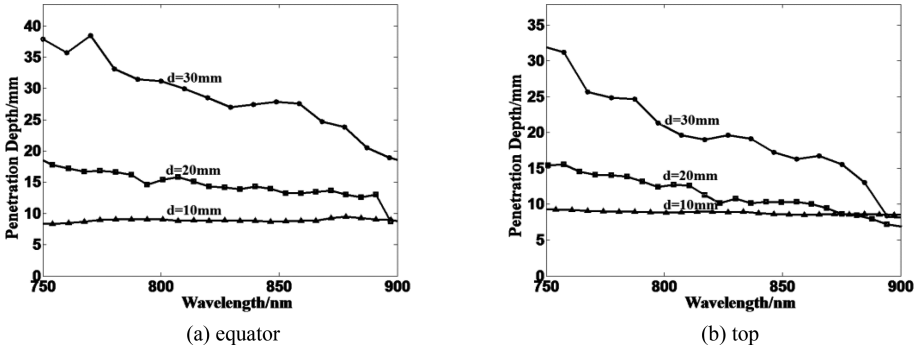


Fig. 5. The penetration depth curves in effective wavelength range

Table 1 shows the penetration depth range and wavelength to largest penetration depth with different source-detector distance on the equator and top. The wavelengths to largest penetration depth are all in the range of 750–800 nm, indicating the NIR light in this range being low absorption feature. And the penetration depth increases with source-detector distance increasing on the equator and top, as is according to Monte Carlo model [14].

4 Conclusions

In this paper, the diffused transmission spectra in the range of 750–900 nm were collected with removing the sample slices. And the penetration depth curves of equator and top were fitted by partial least square method. Results showed that, the penetration depth increased with source-detector distance increasing, and more information about internal quality could be carried by spectra. However, the intensity of spectra was weaker. The transportation feature made little difference between equator and top, but the penetration depth on the top was less than the equator. The result is helpful to design a reasonable source-detector distance for achieving effective penetration depth. And it can provide reference for developing portable and non-destructive device for large fruit.

Acknowledgment. The authors sincerely acknowledge the support by Beijing Municipal Natural Science Foundation (No. 6144024), and Beijing Academy of Agriculture and Forestry Sciences Foundation for Young Scholars (QNJJ201423).

References

1. Tian, H., Ying, Y., Lu, H., et al.: Study on predicting firmness of watermelon by Vis/NIR diffuse transmittance technique. *Spectrosc. Spectral Anal.* **27**(6), 1113–1117 (2007)
2. Zhang, F., Wang, Q., Ma, Z., et al.: Content determination of sugar and fiber in watermelon by near-infrared spectroscopy. *Food Sci.* **28**(1), 258–261 (2007)
3. Jie, D., Xie, L., Rao, X., et al.: Using visible and near infrared diffuse transmittance technique to predict soluble solids content of watermelon in an on-line detection system. *Postharvest Biol. Technol.* **90**, 1–6 (2014)
4. Tian, H.Q., Wang, C.G., Zhang, H.J., et al.: Measurement of soluble solids content in melon by transmittance spectroscopy. *Sens. Lett.* **10**(1–2), 570–573 (2012)
5. Abebe, A.T.: Total sugar and maturity evaluation of intact watermelon using near infrared spectroscopy. *J. Near Infrared Spectrosc.* **14**(1), 67–70 (2006)
6. Li, Y., Zhao, H., Chang, D., et al.: Maturity qualitative discrimination of small watermelon fruit. *Spectrosc. Spectral Anal.* **32**(6), 1526–1530 (2012)
7. Qin, J.W., Lu, R.F.: Monte Carlo simulation for quantification of light transport features in apples. *Comput. Electron. Agric.* **68**(1), 44–51 (2009)
8. Chen, P., Nattuvetty, V.R.: Light transmittance through a region of an intact fruit. *Trans. ASAE* **23**(2), 519–522 (1980)
9. Lammertyn, J., Peirs, A., De Baerdemaeker, J., et al.: Light penetration properties of NIR radiation in fruit with respect to non-destructive quality assessment. *Postharvest Biol. Technol.* **18**, 121–132 (2000)
10. Han, D., Chang, D., Song, S.: Information Collection of mini watermelon quality using near-infrared non-destructive detection. *Trans. Chin. Soc. Agric. Mach.* **44**(7), 174–178 (2013)
11. Fraser, D.G., Jordan, R.B., Künnemeyer, R., et al.: Light distribution inside mandarin fruit during internal quality assessment by NIR spectroscopy. *Postharvest Biol. Technol.* **27**(2), 185–196 (2003)
12. Feng, S.C., Zeng, F., Chance, B.: Monte Carlo simulations of photon migration path distributions in multiple scattering media. In: *SPIE*, vol. 1888, pp. 78–79 (1993)
13. Li, H., Xie, S., Lu, Z., et al.: Visible and near-infrared light scattering model of biological tissue. *Acta Opt. Sin.* **19**(12), 1661–1666 (1999)
14. Wang, L.H., Jacques, S.L., Zheng, L.: Monte Carlo modeling of light transport in multilayered tissues. *Comput. Methods Programs Biomed.* **47**(2), 131–146 (1995)